Effects of the Addition of a Graft Copolymer of Propylene with Styrene on Thermal Behavior, Crystallization, and Morphology of Isotactic Polypropylene

L. D'ORAZIO,[1] R. GUARINO,[1] C. MANCARELLA,[1] E. MARTUSCELLI,[1] G. CECCHIN[2]

[1] Istituto di Ricerca e Tecnologia delle Materie Plastiche del CNR, Via Toiano, 6-80072 Arco Felice, Napoli, Italy

[2] Montell Italia S.p.A, Ferrara, Italy

Received 4 March 1999; accepted 23 May 1999

ABSTRACT: A novel graft copolymer of unsaturated propylene with styrene (uPP-*g*-PS) was added to isotactic polypropylene (iPP) to investigate the state of mixing between uPP-*g*-PS and iPP phase and effects of the uPP-*g*-PS addition on iPP intrinsic phase structure, i.e., on iPP spherulitic texture and inner structure of the spherulites fibrillae. Thin films of iPP/uPP-*g*-PS blends containing 2, 5, and 10% (wt/wt) of graft copolymer were prepared by o-dichlorobenzene casting, according to the method we used previously to obtain samples of iPP/atactic polystyrene/uPP-*g*-PS ternary blends (D'Orazio et al. J Appl Polym Sci 1997, 65, 1539; D'Orazio et al. J Appl Polym Sci, 1999, 72, 1429). The variation of tan δ with temperature and differential scanning calorimetry thermograms showed respectively that, regardless of blend composition, a single glass transition temperature and a single apparent melting temperature were found for the iPP phase in the iPP/uPP-*g*-PS binary systems. Optical microscopy investigation revealed that, with increasing uPP-*g*-PS content, iPP spherulites become more open and coarse. On the other hand, both dimension and number per unit area of the amorphous interspherulitic contact regions decreased. The long period values of the iPP phase, calculated from the peak position of Lorentz-corrected desmeared small angle X-ray scattering profiles, increased markedly with increasing uPP-*g*-PS content; such an increase was due to an increase of both average crystalline lamellar thickness and interlamellar amorphous phase. © 2000 John Wiley & Sons, Inc. J Appl Polym Sci 75: 553–565, 2000

Key words: polypropylene; propylene-*g*-styrene copolymer; blends; morphology; structure; crystallization

INTRODUCTION

In previous articles,[1,2] we reported on results of an investigation aimed at compatibilizing blends of isotactic polypropylene (iPP) and atactic polystyrene (aPS) by means of the addition of a novel graft copolymer of unsaturated propylene with styrene (uPP-*g*-PS). From the previous articles,[1,2] it has been demonstrated that the addition of uPP-*g*-PS copolymer provides iPP/aPS compatibilized materials; the uPP-*g*-PS copolymer forming a coating layer around the aPS particles or interpenetrating the two homopolymer phases depending on a combination of composition and undercooling. Moreover, evidence of a strong correlation between the crystallization process of propylenic sequences of the uPP-*g*-PS copolymer and the iPP crystallization process have been shown.

To achieve a better understanding of both the state of mixing between uPP-*g*-PS and iPP phase

Correspondence to: L. D'Orazio.

Journal of Applied Polymer Science, Vol. 75, 553–565 (2000)
 CCC 0021-8995/00/040553-13

Table I Molecular Characteristics of the Starting Polymers Together with T_g, T'_m, and X_c

Sample	$\bar{M}_n$ (g/mol)	$\bar{M}_w$ (g/mol)	$\bar{M}_w/\bar{M}_n$	η (dL/g)	% PS (wt/wt)	T_g (°C)	T'_m (°C)	X_c
iPP	78,700	509,000	6.5	2.0	—	−9 11	168	0.52
uPP-*g*-PS	—	—	—	1.4	35	118	142	0.22

and of the modifications induced by the addition of the uPP-*g*-PS copolymer on the iPP intrinsic phase structure, that is on iPP spherulitic texture and inner structure of the spherulites fibrillae, samples of binary iPP/uPP-*g*-PS blends have been prepared. Following the method previously used to prepare the samples of the iPP/aPS/uPP-*g*-PS ternary blends,[1] iPP alone and uPP-*g*-PS components have been dissolved in a common solvent, o-dichlorobenzene, and film samples of iPP/uPP-*g*-PS binary blends have been obtained by o-dichlorobenzene casting.

Dynamic mechanical thermal analysis (DMTA), differential scanning calorimetry (DSC), optical microscopy (OM), scanning electron microscopy (SEM), wide angle X-ray scattering (WAXS), and small angle X-ray scattering (SAXS) techniques have been used to investigate thermal behavior, crystallization process, and morphology and structure of iPP/uPP-*g*-PS blends containing 2, 5, and 10% (wt/wt) of copolymer.

The dependence of thermal, morphological, and structural parameters of phases and interphases on composition in film samples of the binary iPP/uPP-*g*-PS systems have been investigated also.

EXPERIMENTAL

Materials

The starting polymers used in this study were an iPP (HS005) made by Himont and a uPP-*g*-PS copolymer synthesized in the Himont Scientific Laboratories according to methods patented by Cecchin and associates from Himont.[4,5] The molecular characteristics of the plain starting materials, together with their glass transition temperature (T_g), apparent melting temperature (T'_m), and crystallinity index (X_c), are reported in Table I.

Blending and Sample Preparation

All the investigated samples were obtained by means of the solvent-casting method already used to prepare the iPP/aPS/uPP-*g*-PS ternary blends.[1,2] The pure components and their blends were dissolved in a common solvent, o-dichlorobenzene at a total polymer concentration of 3% by weight and at a temperature of 135°C. Thin films were obtained by o-dichlorobenzene casting performed under vacuum at 135°C for 3 h. iPP/uPP-*g*-PS binary blends containing 2, 5, and 10% (wt/wt) of graft copolymer were prepared.

Techniques

DSC

The thermal behavior, of thin films of plain starting components and blends as obtained by casting, was analyzed by means of a differential scanning calorimeter with a Mettler TA 3000 equipped with a control and programming unit (microprocessor Tc 10). The apparent T'_m and the X_c were determined following this procedure: the samples (≈10 mg) were heated from room temperature to 200°C at a rate of 10°C/min and the heat evolved during the scanning process was recorded as a function of the temperature. The observed T'_m and the apparent enthalpies of melting (ΔH*) were obtained from the maxima and the area of the melting peaks, respectively. The X_c of the iPP and the blends were calculated by applying the following relations:

$$X_c(\text{iPP}) = \Delta H^*(\text{iPP})/\Delta H^\circ(\text{iPP}) \quad (1)$$

$$X_c(\text{blend}) = \Delta H(\text{blend})/\Delta H^*(\text{iPP}) \quad (2)$$

where ΔH*(iPP) is the apparent enthalpy of fusion per gram of iPP in the blend; ΔH°(iPP) is the heat of fusion per gram of 100% crystalline iPP, from Brandrup and Immergut[6] ΔH°(iPP) = 209 J/g and ΔH* (blend) is the apparent enthalpy of fusion per gram of blend. The crystalline weight fraction referred to the iPP phase in blends [X_c (iPP)]were calculated from the following relation:

$$X_c(\text{iPP}) = X_c(\text{blend})/W(\text{iPP}) \quad (3)$$

where W (iPP) is the weight fraction of iPP in the blends.

The effect of nucleating ability of uPP-*g*-PS copolymers on the crystallization process of iPP was investigated following this procedure: the samples were heated to 200°C with a rate of 10°C/min and kept at this temperature for 10 min to destroy any traces of crystallinity and then cooled with a rate of 10°C/min.

DMTA

The tan δ and storage modulus of all investigated samples were measured by means of a dynamic mechanical thermal analyzer (Rheometric Scientific MK III). Test data were collected in tensile mode from −40 to 140°C using a scanning rate of 1.5°C/min and a frequency of 1 Hz.

OM

Thin films of plain starting components and blends were observed by means of OM. A Zeiss optical polarizing microscope fitted with a Linkman hot stage was used; OMs were taken with crossed and parallel polarizers.

SEM

Cryogenically fractured surfaces of thin films of binary blends were observed by means of a Philips XL 20 scanning electron microscope after coating with Gold-Palladium.

WAXS

WAXS studies were performed by means of a PW 3020/00 Philips diffractometer (CuKα Ni-filtered radiation) equipped with holder for sample spinning; the high voltage was 40 kV and the tube current was 30 mA. A standard sample was used to determine the instrumental broadening.

SAXS

SAXS studies were performed by means of a compact Kratky camera equipped with a Braun one-dimensional positional sensitive detector. Ni-filtered CuKα radiation generated from a Philips X-ray generator (PW 1730/10) operating at 40 kV and 30 mA, was used. They were scattered for parasitic scattering, absorption, and slit smearing by using Vonk's method.[7] The desmeared intensities were then Lorentz factor corrected by multiplying by s^2 ($s = 2 \sin \theta/\lambda$).[8]

Table II T_g, T'_m, X_c of iPP/uPP-*g*-PS Blends [X_c (blend)], Together with X_c of iPP Phase [X_c (iPP)]

Sample	T_g (°C)	T'_m (°C)	X_c (blend)	X_c (iPP)
iPP/uPP-*g*-PS 98 : 2 (wt/wt)	−9	172	0.52	0.52
iPP/uPP-*g*-PS 95 : 5 (wt/wt)	−9	165	0.50	0.51
iPP/uPP-*g*-PS 90 : 10 (wt/wt)	−10 105	165	0.47	0.49

RESULTS AND DISCUSSION

Thermal Behavior

The T_g, detected by DMTA measurements for all the iPP/uPP-*g*-PS blends, are reported in Table II. The variation of tan δ with temperature obtained for such binary systems shows that, regardless of blend composition, a single T_g is found to be ascribed to the iPP phase; such T_g value can be considered within the experimental error to be the same T_g value as the plain iPP.[1,2]

The DSC thermograms of the binary iPP/uPP-*g*-PS blends investigated show a single endothermic peak of iPP phase when heated from room temperature to 200°C. Noteworthy is that such a peak sharpens with uPP-*g*-PS addition and that the extent of such an effect is composition-dependent; the observed sharpening, in fact, increases on increasing the uPP-*g*-PS content [see Fig. 1(a)]. Such findings could suggest comparatively higher perfection and/or narrower size distribution of the lamellar crystals of iPP phase on increasing the uPP-*g*-PS content. The temperatures corresponding to the maxima of the peaks (T'_m) are reported in Table II together with the crystallinity indices of the blends [X_c (blend)] and of the iPP phase [X_c (iPP)]. As shown, there is no systematic dependence of the T'_m values on blend composition, whereas both X_c (blend) and X_c (iPP) values decrease with increasing copolymer content. It is interesting to recall that the DSC thermogram of plain uPP-*g*-PS copolymer shows a double melting peak, the first being broader and lower than the second. The temperature positions of such peaks are reported in Table I and are considerably lower than that shown by the iPP phase. Taking into account that, regardless of copolymer content, no separate melting of the uPP-*g*-PS propylenic sequences is detected in the

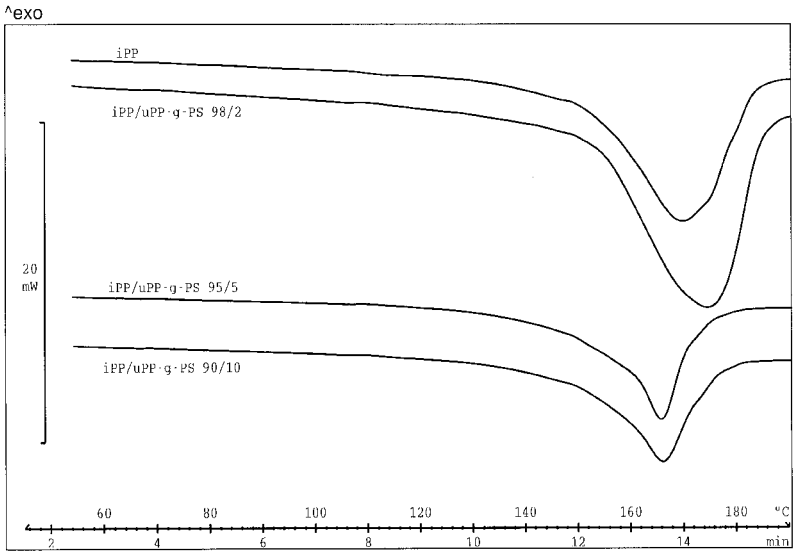
^exo
iPP
iPP/uPP-g-PS 98/2
20
mW
iPP/uPP-g-PS 95/5
iPP/uPP-g-PS 90/10
60 80 100 120 140 160 180 °C
2 4 6 8 10 12 14 min

a)

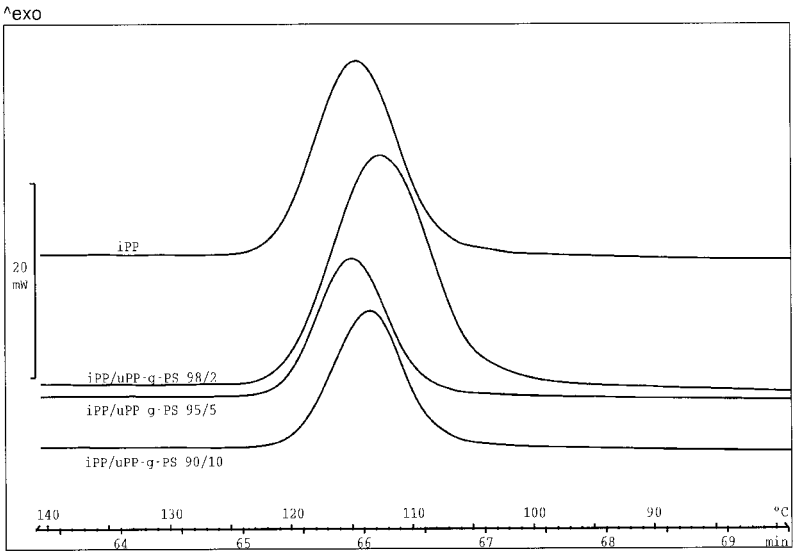
^exo
20
mW
iPP
iPP/uPP-g-PS 98/2
iPP/uPP g-PS 95/5
iPP/uPP-g-PS 90/10
140 130 120 110 100 90 °C
64 65 66 67 68 69 min

b)

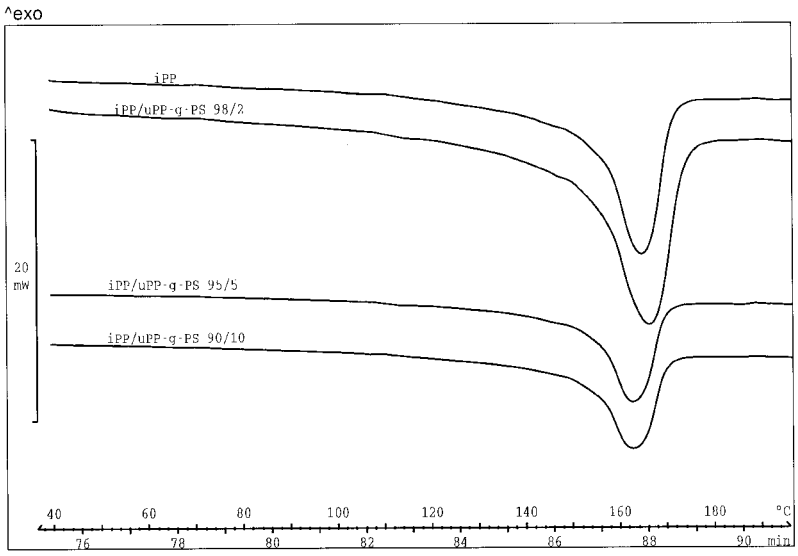
^exo
iPP
iPP/uPP-g-PS 98/2
20
mW
iPP/uPP-g-PS 95/5
iPP/uPP-g-PS 90/10
40 60 80 100 120 140 160 180 °C
76 78 80 82 84 86 88 90 min

c)

DSC traces of the iPP/uPP-*g*-PS samples, it could be that such sequences are able to cocrystallize with iPP thus allowing the formation of crystalline phases with different perfection and/or thicknesses.

The curve of nonisothermal crystallization from melt of the plain iPP is compared with those shown by the iPP phase nonisothermally crystallized from melts of the binary iPP/uPP-*g*-PS blends in Figure 1(b). As shown, when the iPP crystallizes in the presence of uPP-*g*-PS copolymer, regardless of blend composition, the range of crystallization temperature remains comparable to that shown by the plain iPP, indicating that uPP-*g*-PS copolymer has no nucleating ability on the crystallization process of the iPP. In other words, such a copolymer does not contain heterogeneous nuclei that migrate toward the iPP phase and the nucleation density of the iPP phase is independent of composition. Such results agree with previous results related to iPP/aPS/uPP-*g*-PS ternary systems.[1] Noteworthy also is that the uPP-*g*-PS copolymer shows a range of nonisothermal crystallization fully included in that shown by the plain iPP, indicating that its crystallization process from the melt is strictly correlated with that of the plain iPP.

The DSC thermograms of nonisothermally crystallized samples of iPP and its binary blends are shown in Figure 1(c); a single endothermic peak, when heated from room temperature to 200°C, is exhibited by all the investigated samples in agreement with the thermal behavior shown by the samples obtained from solution-casting. The temperature position of the maxima of the observed peaks (T'_m), X_c (blend), and X_c (iPP) values are reported in Table III; the trend of such data agrees with that found for the cast samples although, owing to the crystallization condition imposed, such values are lower than that shown by the iPP phase in the solution-cast samples (compare Tables II and III).

Table III Nonisothermal Crystallization Range for Plain iPP and uPP-*g*-PS Copolymer and for iPP Nonisothermally Crystallized from iPP/uPP-*g*-PS Blends Together with T'_m, X_c (blend), and X_c of iPP Phase [X_c(iPP)]

Sample	Nonisothermal Crystallization Range (°C)	T'_m (°C)	X_c (blend)	X_c (iPP)
iPP	127 ÷ 96	163	0.45	0.45
iPP/uPP-*g*-PS 98 : 2 (wt/wt)	127 ÷ 96	164	0.42	0.42
iPP/uPP-*g*-PS 95 : 5 (wt/wt)	126 ÷ 99	161	0.42	0.42
iPP/uPP-*g*-PS 90 : 10 (wt/wt)	127 ÷ 95	162	0.41	0.43
uPP-*g*-PS	117 ÷ 89	139	0.22	0.34

Phase Structure

Microscopy Studies in Solid and Melt State

Figure 2 shows optical micrographs, taken at crossed and parallel polarizers, of thin films of the plain iPP, which, as expected, exhibits a regular spherulitic superstructure with large amorphous interspherulitic contact regions in agreement with previous results.[1,2] Crossed and parallel polarizers OMs of the iPP/uPP-*g*-PS blends are shown in Figure 3. For low copolymer content, the iPP phase crystallizes forming spherulites in which size, neatness, and regularity are comparable to that shown by the plain iPP. Moreover, spherical-shaped domains are occluded in the iPP intraspherulitic regions and there are some amorphous interspherulitic contact regions. With increasing uPP-*g*-PS content (wt/wt), the iPP spherulites tend to become more open and coarse; such an effect is composition dependent. Comparatively more open and coarse spherulites are in fact exhibited by the blends containing the highest uPP-*g*-PS content (see Fig. 3) suggesting that the amount of uncrystallizable material located in interfibrillar and interlamellar regions of iPP crystals increases with increasing uPP-*g*-PS content. Moreover, both dimension and number per unit area of the amorphous interspherulitic contact regions decrease with increasing uPP-*g*-PS content, indicating that the rejection phenomenon of uncrystallizable material from the iPP crystal front becomes less pronounced on enhancing copolymer content. The morphological results

Figure 1 Thermal behavior of plain iPP and iPP/uPP-*g*-PS blends: (a) DSC thermograms of plain iPP and iPP/uPP-*g*-PS blends containing 2, 5, and 10% (wt/wt) of uPP-*g*-PS copolymer; (b) Nonisothermal crystallization curves for plain iPP (a) and for iPP phase crystallized from iPP/uPP-*g*-PS blends containing 2, 5, and 10% (wt/wt) of uPP-*g*-PS copolymer; (c) DSC thermograms of nonisothermal crystallized samples of plain iPP and iPP/uPP-*g*-PS blends containing 2%, 5%, and 10% (wt/wt) of uPP-*g*-PS copolymer.

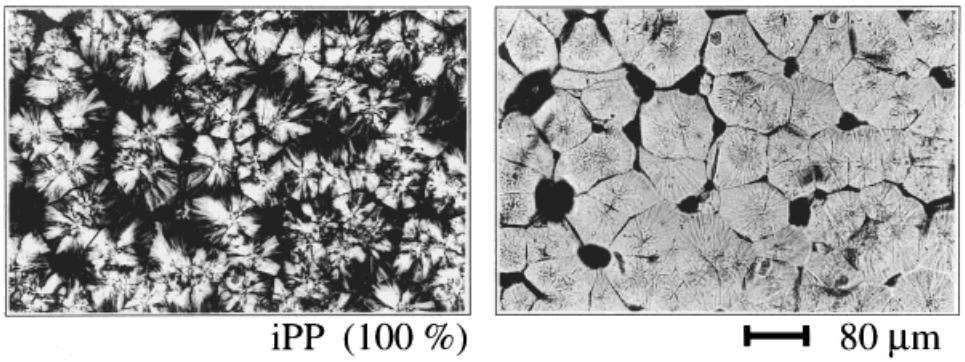

Figure 2 OMs taken at crossed and parallel polarizers of thin films of plain iPP.

obtained can be accounted for by hypothesizing that the decreased rejection phenomenon is to be related to different states of mixing of the blend components, i.e., to miscibility effects in the amorphous state among propylenic sequences of the uPP-*g*-PS copolymer and iPP depending on com-

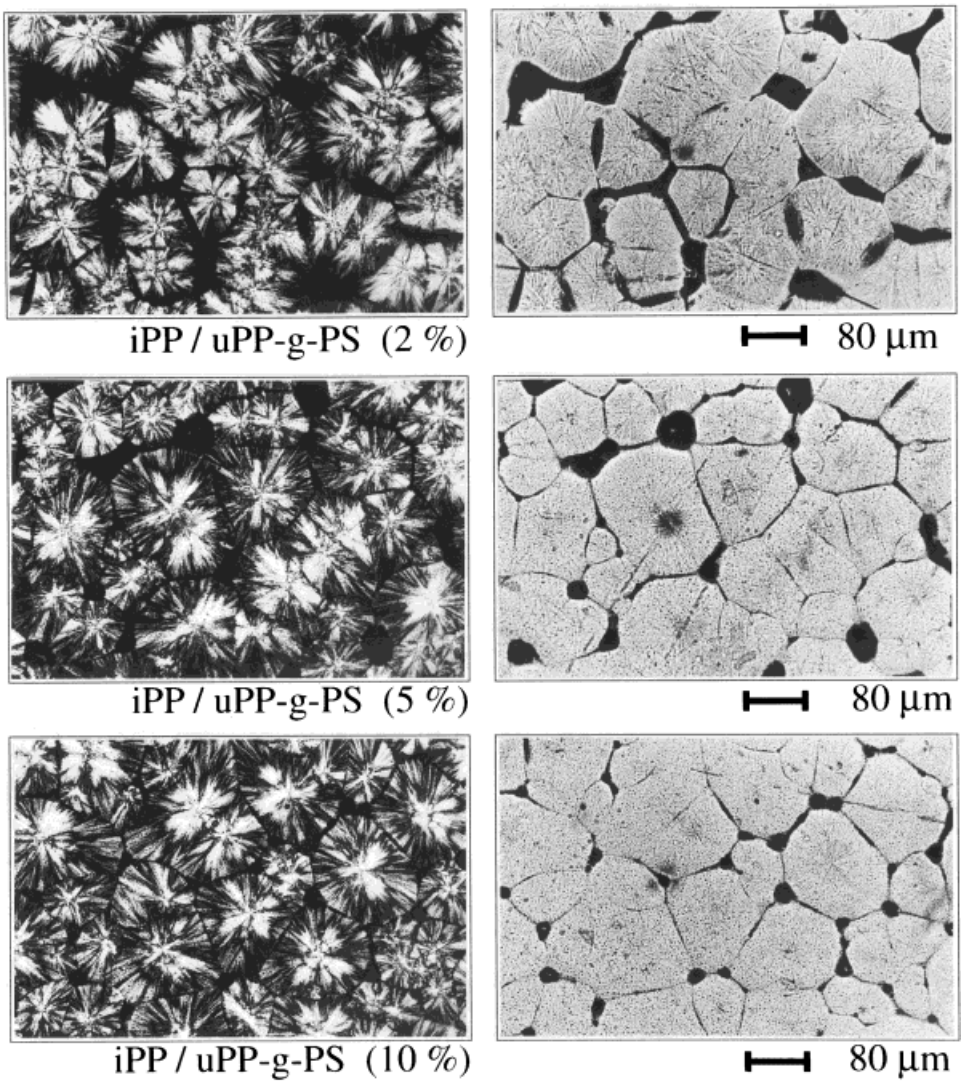

Figure 3 OMs taken at crossed and parallel polarizers of thin films of iPP/uPP-*g*-PS blends containing 2 (a), 5 (b), and 10% (wt/wt) (c) of uPP-*g*-PS copolymer.

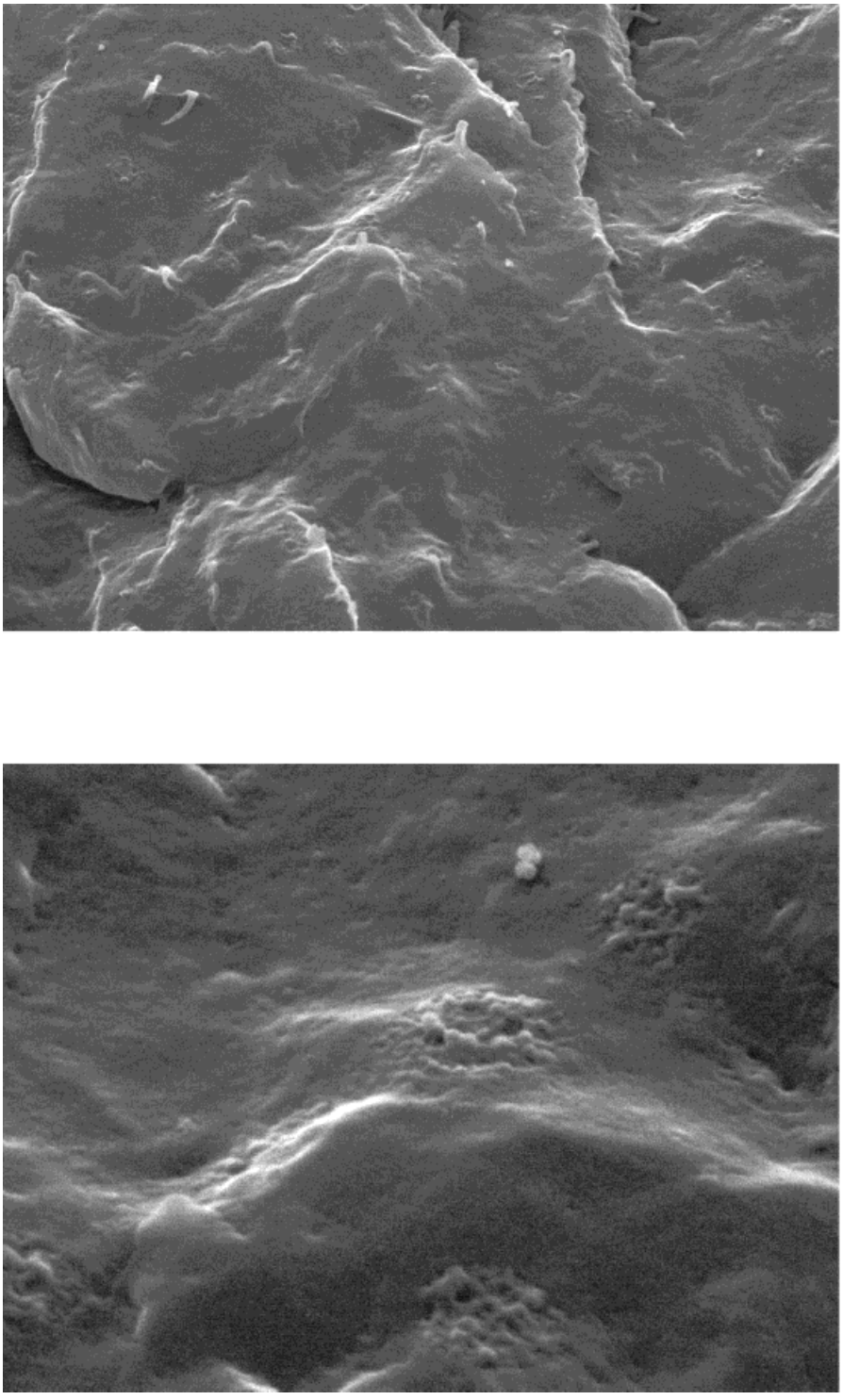

Figure 4 SEMs of cryogenically fracture surfaces of thin films of iPP/uPP-*g*-PS blends 90/10 (wt/wt), original magnification ×10,000 (a) and ×20,000 (b).

position. Owing to such effects, propylenic sequences of the uPP-*g*-PS copolymer could be occluded by the crystallizing front in the interlamellar regions and/or in interfibrillar regions of the iPP crystals according to their chemical constitution and configurational regularity. From the

SEM investigation performed on cryogenically fractured surfaces of iPP/uPP-*g*-PS films, all the materials exhibit such a homogeneous texture that domains of dispersed phase can be clearly detected only at very high magnification (×20,000). Particles in which maximum diameter is lower than 0.5 μm and no holes where such particles separated can be observed (see Fig. 4).

OMs taken at parallel polarizers of thin films of iPP/uPP-*g*-PS blends melted at the temperature of 200°C, and kept at this temperature for 10 min to destroy any crystallinity trace, are reported in Figure 5. As shown, the iPP/uPP-*g*-PS melts are not homogeneous notwithstanding DMTA experiments showing a single T_g for the iPP phase; dispersed phase domains are in fact observed even for low uPP-*g*-PS content (2% wt/wt). Such domains are spherically shaped, have small size and show, by visual impressions, narrow size distribution indicating low interfacial tension between iPP and uPP-*g*-PS melts (see Fig. 5). To be observed is that with enhancing copolymer content from 5 to 10 % (wt/wt), a comparatively finer and more homogeneous dispersion degree of minor component is achieved; as a matter of fact, the number of domains of dispersed phase per unit area increases, suggesting a state of mixing of uPP-*g*-PS copolymer with iPP depending on composition.

Figure 6 shows OMs taken at crossed and parallel polarizers of films quenched from the melt state of plain iPP and iPP/uPP-*g*-PS blends. As shown, microspherulitic texture and very fine and homogeneous dispersion of minor component, regardless of blend composition, is achieved. The comparison between the melt morphologies of the iPP/uPP-*g*-PS blends with the morphologies generated after quenching (compare Fig. 2 and 6) surprisingly shows that the iPP crystallization process provides interconnected materials more homogeneous than corresponding melts, as reduced particle size and narrowed particle size distribution are found. Noteworthy is that the higher the copolymer content, the finer is the dispersion degree of minor component. Moreover, no amorphous interspherulitic contact regions are observed irrespective of uPP-*g*-PS content (wt/wt) (see Fig. 6).

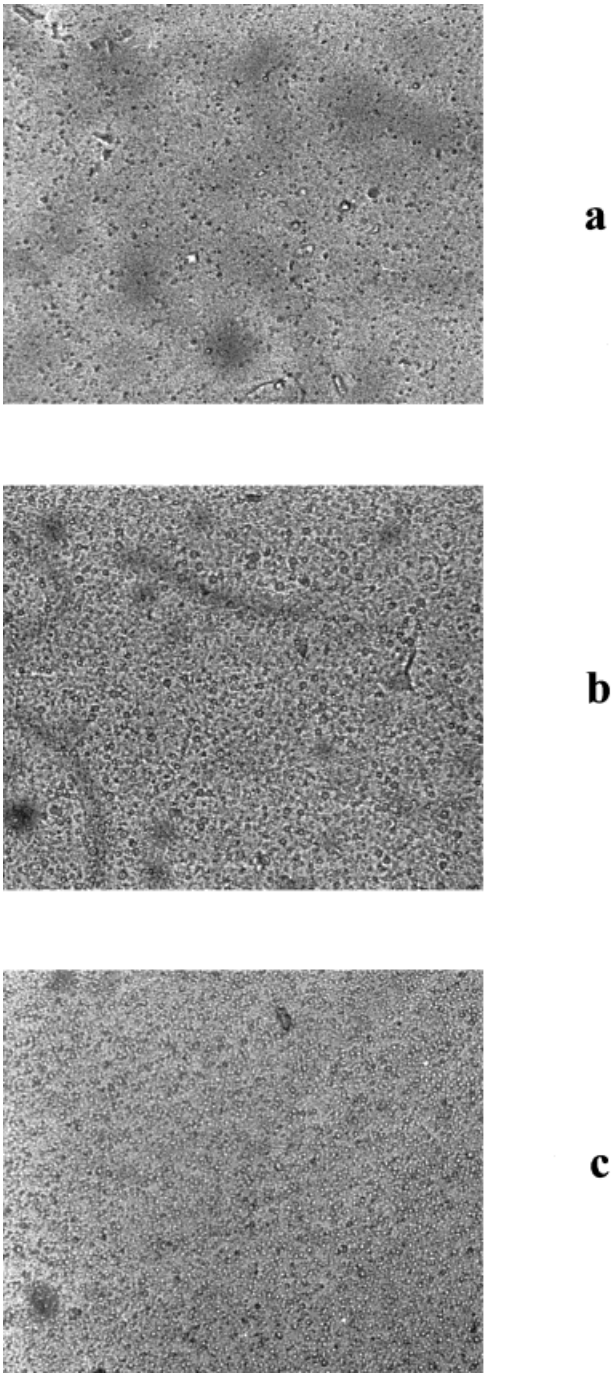

Figure 5 OMs taken at parallel polarizers of thin films of iPP/uPP-*g*-PS blends containing 2 (a), 5 (b), and 10% (wt/wt) (c) of uPP-*g*-PS copolymer melted at the temperature of 200°C.

WAXS Studies

Typical WAXS diffractograms of thin films of plain iPP and iPP/uPP-*g*-aPS blends are shown in Figure 7. As shown, all the samples give diffraction peaks in which angles are characteristic for the crystal structure of the α form of polypropylene and, in addition show a broad, diffraction, noncrystalline halo centred at 2θ values equal to $17.4 \pm 0.1°$.

The apparent crystal size (D) of iPP in the perpendicular direction to the (110), (040), and

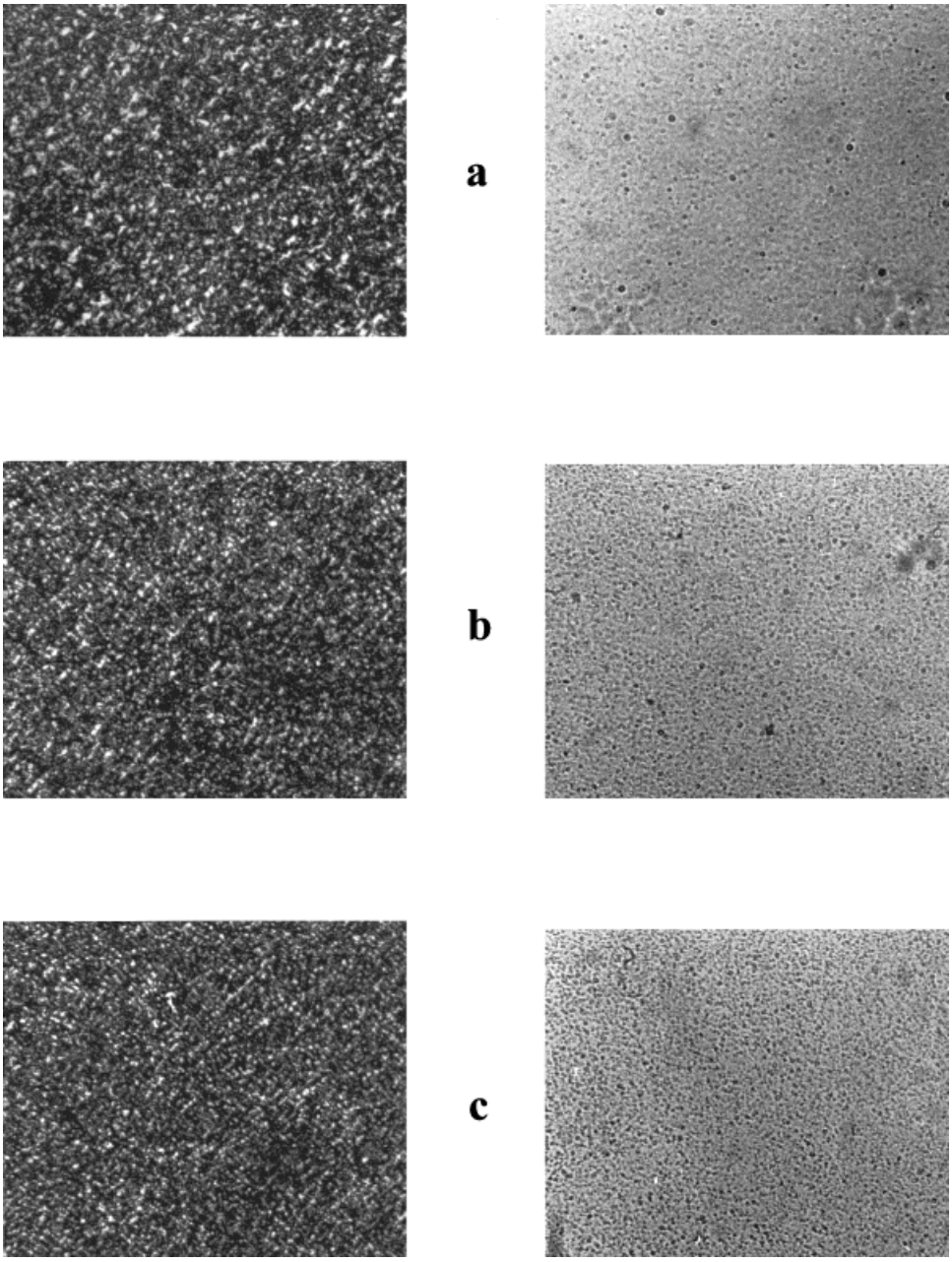

Figure 6 OMs taken at crossed and parallel polarizers of quenched samples of iPP/uPP-*g*-PS blends containing 2 (a), 5 (b), and 10% (wt/wt) (c) of uPP-*g*-PS copolymer.

(130) crystallographic planes was calculated by the Sherrer equation[8]:

$$D_{hkl} = K\lambda/\beta_0\cos(\theta_{hkl}) \quad (4)$$

where β_o is the half-width in radians of reflection corrected for instrumental broadening, and λ is the wavelength of the radiation used (1.5418 å). The shape factor K is set equal to unity, so the size data have to be considered as relative data. The apparent crystal sizes (D) of the iPP phase crystallized in the presence of uPP-*g*-PS copolymer are higher than that of the plain iPP indicating a higher growth of the iPP crystals in the blends (see Table IV). Noteworthy is the dependence on composition of the D values; such values increase with increasing uPP-*g*-PS content. Assuming that the folding surface of the iPP lamel-

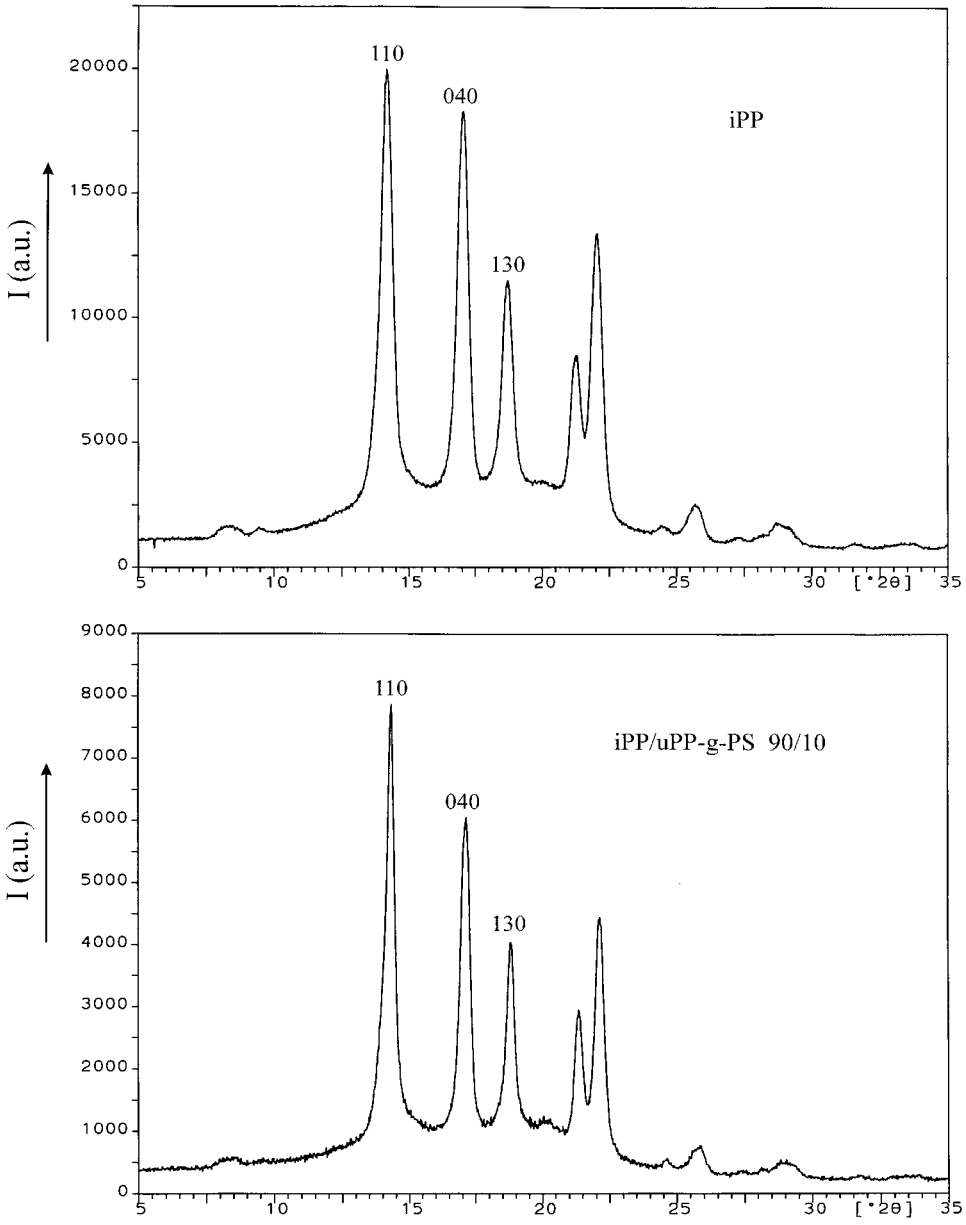

Figure 7 WAXS diffractograms of films of plain iPP and iPP/uPP-*g*-PS blends 90:10 (wt/wt).

lar crystals is perpendicular to the *c* axis of the iPP monoclinic unit cell, the $D_{(110)}/D_{(040)}$ ratio represents the ratio between the apparent crystal size in direction parallel to the a^* axis (the a^* axis being the radial growth direction of the spherulites) and the apparent crystal size in direction parallel to the *b* axis (D_{a^*}/D_b). D_{a^*}/D_b ratio values almost constant within the experimental error indicate therefore that the iPP phase crystallized in the presence of uPP-*g*-PS copolymer does not form comparatively thicker lamellae in the direction of the spherulites radial growth in line with DSC results, i.e., with a number of nuclei for iPP volume unit and consequently crystal growth occurring at undercooling comparable to that of the plain iPP.

SAXS Studies

Typical Lorentz-corrected desmeared profiles for samples of plain iPP and iPP/uPP-*g*-PS blends are shown in Figure 8. These SAXS profiles exhibit

Table IV Apparent Crystal Size (D) of Plain iPP and iPP/uPP-*g*-PS Blends Together with the Ratio Between $D_{(110)}$ and $D_{(040)}$

Sample	$D_{(110)}$ (Å)	$D_{(040)}$ (Å)	$D_{(130)}$ (Å)	$D_{(110)}/D_{(040)}$
iPP	88	96	106	0.92
iPP/uPP-*g*-PS 98 : 2 (wt/wt)	105	112	105	0.94
iPP/uPP-*g*-PS 95 : 5 (wt/wt)	105	117	119	0.90
iPP/uPP-*g*-PS 90 : 10 (wt/wt)	100	112	112	0.89

well-defined maxima; by applying Bragg's law, the long period (L) of the iPP phase has been calculated from the peak position. It is very interesting to observe that the peak position shifts to lower angles with increasing uPP-*g*-PS content in the blends. Assuming a two-phase model for the iPP spherulite fibrillae, consisting of alternating parallel crystalline lamellae and amorphous layers, the crystalline lamellar thickness (L_c) has been calculated using the following relation for the L values:

$$L_c = \frac{X_{c\,(\mathrm{iPP})} \cdot L}{(\rho_c/\rho_a)(1 - X_{c\,(\mathrm{iPP})}) + X_{c\,(\mathrm{iPP})}} \qquad (5)$$

where $X_{c\,(\mathrm{iPP})}$ is the DSC crystallinity index of the iPP phase; and ρ_c and ρ_a are the densities of the crystalline and amorphous iPP phases, respectively.

The thickness of the amorphous interlamellar layer (L_a) has been calculated by:

$$L_a = L - L_c \qquad (6)$$

The L, L_c, and L_a of the plain iPP and iPP/uPP-*g*-PS blends are reported in Table V. As shown, L values increase markedly with increasing uPP-*g*-PS content indicating the presence of uPP-*g*-PS phase between iPP lamellae. According to rela-

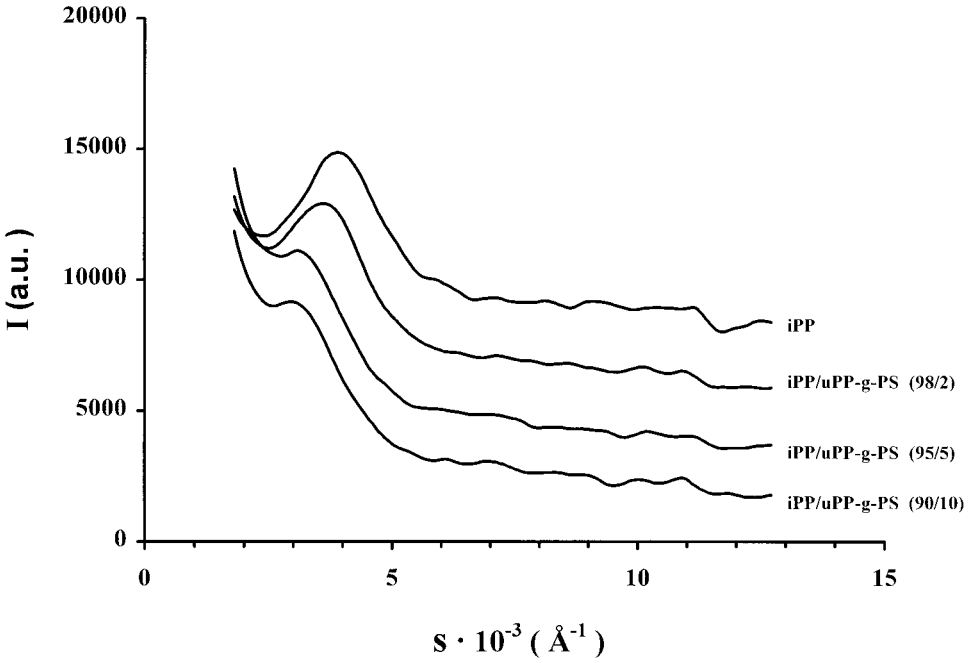

Figure 8 Typical SAXS Lorentz-corrected desmeared profiles for samples of plain iPP and iPP/uPP-*g*-PS blends containing 2, 5, and 10% (wt/wt) of uPP-*g*-PS copolymer.

Table V Long Period (L), Crystalline Lamella Thickness (L_c), and Interlamellar Amorphous Thickness (L_a) for Plain iPP and Its Blends

Sample	L (Å)	L_c (Å)	L_a (Å)
iPP	256	127	129
iPP/uPP-*g*-PS 98 : 2 (wt/wt)	279	138	141
iPP/uPP-*g*-PS 95 : 5 (wt/wt)	325	158	167
iPP/uPP-*g*-PS 90 : 10 (wt/wt)	339	158	181

tions [5] and [6], the noticeable increase of L with uPP-*g*-PS composition is due to the increase of both the average crystalline thickness and interlamellar amorphous phase (see Table V and trends of plots of Fig. 9). Thus, when iPP crystallizes in the presence of uPP-*g*-PS copolymer, the phase structure developed in the blends results in lamellar thickness and in interlamellar amorphous layer higher than that shown by the plain iPP and higher with increasing uPP-*g*-PS content. Assuming on the basis of the evidence thus far obtained that the aPS sequences of the uPP-*g*-PS copolymer tend to be mainly rejected by the iPP crystallizing front in interfibrillar regions, the observed increase in both L_c and L_a values can be accounted for by the occurrence of a cocrystallization phenomenon among propylenic sequences of uPP-*g*-PS copolymer and iPP. During such a process, it cannot be excluded that aPS chains, probably owing to their shortness,[3] remain entrapped in the iPP interlamellar amorphous regions forming their own domains. Therefore, the development of the iPP lamellar structure can be modeled as a function of the uPP-*g*-PS content according to the schematic model reported in Figure 10. Such conclusions ratify the results of the SAXS investigation performed on solvent cast samples of iPP/aPS/uPP-*g*-PS ternary blends.[1]

CONCLUSIONS

A study aimed at investigating the state of mixing between iPP and uPP-*g*-PS phase and morphology and structure of the iPP phase in samples of iPP/uPP-*g*-PS blends has been performed. To be noted is that:

- iPP/uPP-*g*-PS melts are phase separated and therefore the growth of iPP crystal starts from nonhomogeneous systems, notwithstanding the variation of tan δ with temperature of iPP/uPP-*g*-PS blends exhibits a single T_g of iPP phase, in which the value is that of plain iPP T_g.
- No separate melting of uPP-*g*-PS propylenic sequences is shown by the DSC traces of iPP/uPP-*g*-PS blends irrespective of composition.
- iPP phase crystallized in the presence of uPP-*g*-PS copolymer shows X_c lower than that shown by plain iPP on enhancing copolymer content.
- iPP phase crystallizes in a spherulitic superstructure with spherical-shaped domains of dispersed phase occluded in intraspherulitic regions; the average maximum diameter of particles evaluated by SEM being lower than 0.5 μm. With increasing uPP-*g*-PS content such spherulites become more open and coarse and the dimension and number per unit area of the amorphous interspherulitic contact regions decrease.
- The phase structure developed in iPP/uPP-*g*-PS systems is characterized by lamellar thickness (L_c) and interlamellar amorphous layer (L_a) higher than that shown by the plain iPP and higher with increasing uPP-*g*-PS content.

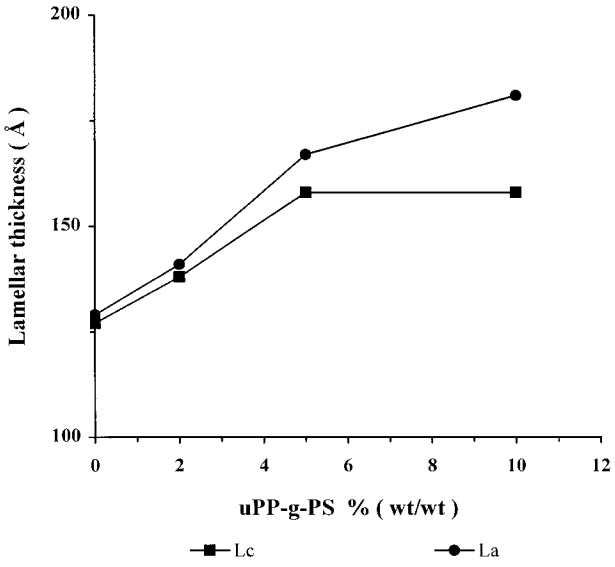

Figure 9 Plots of the lamellar thickness of iPP phase as a function of uPP-*g*-PS content.

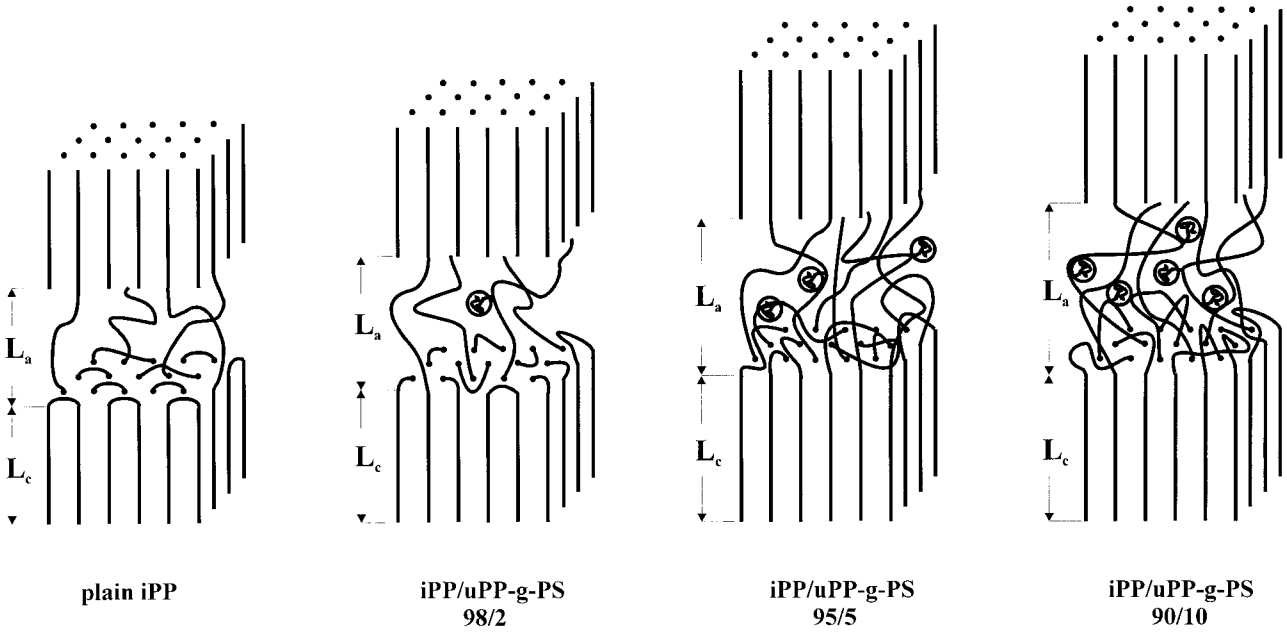

Figure 10 Schematic models of the lamellar structure of plain iPP and iPP phase crystallized in the presence of 2, 5, and 10% (wt/wt) of uPP-*g*-PS copolymer.

The results obtained thus far have been accounted for by the occurrence of both miscibility effects in the amorphous state among propylenic sequences of uPP-*g*-PS phase and iPP and of a cocrystallization phenomenon of copolymer propylenic sequences and iPP.

Work is in progress to establish the influence of the crystallization conditions on morphology of phase and interphase developed after complete crystallization from the melt state under controlled crystallization conditions in film samples of iPP/uPP-*g*-PS blends isothermally crystallized at relatively low undercooling in a range of crystallization temperature of the iPP phase.

REFERENCES

1. D'Orazio, L.; Guarino, R.; Mancarella, C.; Martuscelli, E. J Appl Polym Sci 1997, 65, 1539.
2. D'Orazio, L.; Guarino, R.; Mancarella, C.; Martuscelli, E. J Appl Polym Sci 1999, 72, 1429.
3. D'Orazio, L.; Mancarella, C.; Martuscelli, E.; Sticotti, G. J Mater Sci 1995, 30, 4960.
4. Cecchin, G.; Guglielmi, F.; Zerega, F. U.S. Pat. 4, 602, 077, 1986.
5. Cecchin, G.; De Nicola, A. U.S. Pat. 5, 159, 023, 1990.
6. Brandrup, S.; Immergut, E. M. Polymer Handbook; Interscience: New York, 1975; Vol. 5.
7. Vonk, C. G. J Appl Crystallogr 1975, 8, 340.
8. Alexander, L. E. X-Ray Diffraction in Polymer Science; Wiley: New York, 1969.